AN INNOVATIVE PHYSICS-BASED MODEL OF PEROVSKITE SOLAR CELLS

Nguyen Tuan Anh, Nguyen Huu Duc*

Abstract: *Perovskites are increasingly proved to be a promising candidate for making absorber materials for high-efficiency and low-cost next-generation solar cells. There are several models proposed for perovskite solar cells similar to the conventional solar cells; their operation also has specific characteristics and requires the development of a more general physical model to study, thus optimizing the cells and improving the performance of the panels. This paper develops such a physics-based intuitive model to consider the performance of two high-efficiency types of perovskite solar cells, taking into account heterogeneous properties, with filtered transport layers, recombination, charge selection, and voltage-dependent collector. This model would allow experimentally to estimate critical parameters of perovskite solar cells, understand the performance bottleneck, and predict the performance of perovskite solar cells and suggest further study for perovskite solar cell technology development.*

Keywords: Perovskites; Solar cell; Physics-based analytical model.

1. INTRODUCTION

The increasing demand for solar power in the world and Viet Nam has promoted the rapid development of solar power cell technology. It can be predicted that solar power will continue to evolve in the coming years. There are two current trends aimed at achieving the best performance. One is to maximize the time facing the sun. A solar tracker that is used can increase performance by up to 20% in winter and 50% in summer. Static systems can be optimized by analyzing the sun's path by adjusting corners for summer or winter. The other trend is the development of solar fabrication materials. It is soon expected to have a so-call "third generation of photovoltaics" with low cost and higher efficiency to replace the old types of solar cells. The one we are looking for is perovskite solar cell (PSC), which offers both high energy conversion efficiency and a lower price. Indeed, since the first use of perovskite in the thin-film transistors and LEDs [1, 2], and then into a novel thin-film solar technology as a bulk solar absorber [3-6], the efficiency of PSCs has increased extremely rapidly from around 3% to above 20% [7]. The development of PSC with advantages in the stability and material properties of PSCs makes the PSC become a scorching topic [8, 9].

A typical PSC can be made using either p-i-n or n-i-p structure, as shown in figure 1, which contains a three-layer architecture consisting of a layer made by perovskite material that plays a role as an absorber (300 ~500 nm) sandwiched between an electron-transport layer (n-type ETL) and a hole-transport layer (p-type HTL). The choices for the n-type layer could be TiO_2, ZnO, PCBM, CdS, etc. The options for p-type layer could be PEDOT:PSS, NiO, P_3HT, Poly-TPD, PTAA, etc. In the traditional structure for p-type layer, PEDOT: PSS is the front hole transport layer, and PCBM is the back electron transport layer. The n-type structure, however, has TiO_2 and Spiro-OMeTAD as the front electron transport layer and the back hole transport layer.

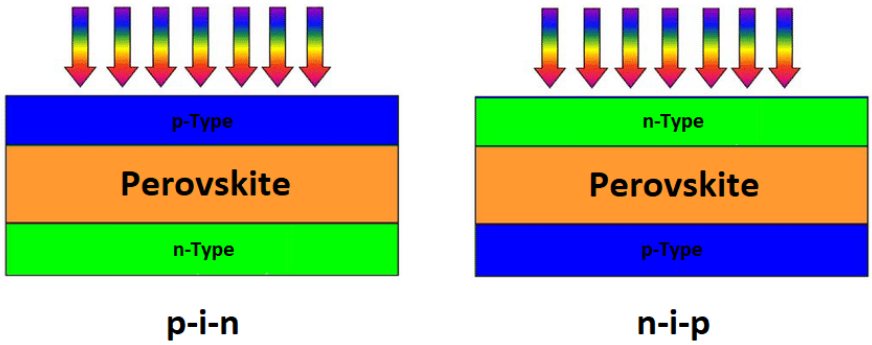

Figure 1. *Device structure of PSCs for p-i-n (left) or n-i-p (right) [15].*

Unlike other solar panels, the ones made from perovskite are able to absorb most of the solar spectrum and act in different atmospheric conditions rather than just under direct sunlight. This type of material works in diffuse conditions much better than other types of solar batteries. The production process of the perovskite panel is very simple, but researchers still have to inspect the material under different conditions to better understand its properties before the companies embark on industrial-scale production.

Understanding the property of perovskite material is the first step for the study of physics, design, optimization, and degradation of PSC. There have been many basic studies first to find out the characteristics of perovskite materials, such as about energy slots, the performance limitation of Shockley-Queisser, defects for various perovskite materials. There are also some attempts to learn the perovskite PV mechanics based on the simulation. However, up to now, most theoretical works have been numerical or empirical [10-14]. Thus, these models still lack rapid characterization and/or estimation of panel performance. Recently, a physics-based analytical model is proposed in [15] in which characterization and optimization of PSC can be done. This model shows the fact that the structure, self-doping, and charge collection in PSC are specific, and cannot be described by traditional approaches, despite a superficial similarity with p-i-n or n-i-p PSCs [16, 17]. However, this model [15] ignores carrier recombination within the absorber layer by considering diffusion length extraordinarily long in perovskite.

In this paper, we develop the model [15] to derive systematically the essential features of perovskite cells based on an analytical model for two types of traditional and inverted structures. We complete the analysis of the operation of PSCs by describing the mechanisms of charge collection, composed of the combination of carrier transport, recombination, and extraction at the selective contacts. We establish the main intuitive ideas concerning the charge collection by either diffusion or by drift in strong electrical fields associated with space-charge regions. The modeling of the solar cell by transport–recombination equations, as well as the boundary conditions. A complex analytical model is reviewed, and then we simulate numerically that allows treating any type of complex morphology of charge and current distribution. We form a basic classification of the main operation modes for charge collection, depending on the size of the depletion region with respect to the thickness of the absorber, environment temperature, and

other parameters. We finish with some practical considerations for the measurement and reporting of solar cell performance and can be easily extended for further studies to optimize and evaluate perovskite-based solar panels and modules [18-22].

This work is set out as follows. In section 2, we describe the mechanisms of charge collection, composed of the combination of carrier transport, recombination, and extraction at the selective contacts by transport–recombination equations and the boundary conditions. The physics quantities and parameters are discussed here. In section 3, simulation results and some discussion are considered. Finally, in section 4, we draw our conclusions.

2. PHYSICAL MODEL

A PSC converts solar energy directly to electric energy. A PSC is mostly made of a p-n junction. The basic operation of a solar cell as follows [15, 23, 24]:

1) *Generation process*: When light enters and is absorbed in a solar cell, free electron-hole pairs are generated. Those electrons and holes will drift, and diffuse will lead to a photo-current when being collected. Therefore, the higher efficiency PSC gets as the higher the generation rate achieves.

2) *Recombination process*: It is the reverse process of a generation when free electrons and holes annihilate each other. The carrier concentration in the solar cell will be reduced during the recombination process; thus, the efficiency of the conversion will be reduced too. Therefore, understanding the recombination process is very much essential to design the solar cell with the minimum rate of recombination.

3) *Carrier transport*: Free carriers that do not participate in the process of recombination will move to the terminals of a solar cell and get collected. Depending on the electric field distribution and carrier concentration distribution, the process of transport can be either dominated by drift or diffusion. A careful design of the transport process in a solar cell is critical to achieving high collection probability and thus high efficiency.

Here we consider a PSC now with a perovskite absorber layer (300 ~ 500 nm), sandwiched between an ETL and an HTL in two types: the traditional structure and the inverted structure, as shown in figure 2. The charge collection mechanism consists of generation, recombination, diffusion, and drift transports. Generation characterized by the optical absorption of perovskite material. Recombination depends on the local density and lifetime of carriers. Drift transport is forced by the electric field of the semiconductor, while diffusion transport is governed by the gradient of carrier concentration in the material.

Thus, in order to analyze the dominant processes of operation of a PSC for charge transport and charge extraction, we will adopt a model in which the carriers obey the general drift-diffusion equations for electrons and holes in a layer $0 \le x \le d$. Therefore, an analysis model can be developed by solving the constant equation of the electron and the hole in the absorbent kit, namely,

$$\partial n/\partial t = -\partial j_n/\partial x + G - R_n, \quad (1)$$

$$\partial p/\partial t = -\partial j_p/\partial x + G - R_p, \quad (2)$$

where n and p are the concentrations of electrons and holes, $G(x)$ and $R_{n(p)}$ the generation and electron (hole) recombination rate, j_n and j_p are electron- and hole-currents, respectively;

$$J_n = -q\,j_n = q\mu_n nE + qD_n\,\partial n/\partial x, \quad (3)$$
$$J_p = +q\,j_p = q\mu_p pE - qD_p\,\partial p/\partial x. \quad (4)$$

Where q is the electric charge, E is the electric field, $D_{n(p)}$ and $\mu_{n(p)}$ are the diffusion coefficient and mobility of electron and hole, respectively.

In a p-doped semiconductor, the majority carrier density p is basically constant, $p \approx p_o$ (except at very high-injection levels), and the electron recombination rate depends only on the local electron density and is often described in terms of the electron lifetime τ_n. And similar to the hole recombination rate,

$$R_n = (n - n_o)/\tau_n,$$
$$R_p = (p - p_o)/\tau_p.$$

Then, the electron and hole continuity equations reduce to

$$D_n\,\partial^2\Delta n/\partial x^2 + \mu_n E\,\partial\Delta n/\partial \mathrm{x} + G(x) - \Delta n/\tau_n = 0, \quad (5)$$
$$D_p\,\partial^2\Delta p/\partial x^2 - \mu_p E\,\partial\Delta p/\partial \mathrm{x} + G(x) - \Delta p/\tau_p = 0, \quad (6)$$

where $\Delta n = n - n_o$ and $\Delta p = p - p_o$.

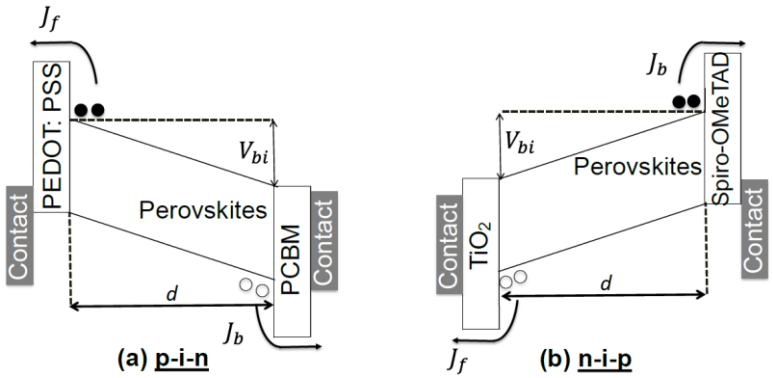

Figure 2. *The energy diagram of (a) p-i-n type and (b) n-i-p type PSCs.*

To solve the equations (5) and (6), we first need to know the generation profile, $G(x)$, by solving the Maxwell equations and find E by solving the Poisson equation.

The carrier generation rate at the position x is given by the attenuation of the photon number, $G(x) = d\Phi_{ph}(x, \lambda)/dx$. Using the Beer-Lambert law and integrating over the wavelength of the incident radiation λ,

$$G(x) = \int (1 - f_R)\sigma(\lambda)\Phi_{ph}(0,\lambda)e^{-\sigma(\lambda)x},$$

where $\Phi_{ph}(x, \lambda)$ is the incident photon number, and f_R is the reflection coefficient. For monochromatic radiation, it is $G(x) = \sigma(\lambda)\,\Phi_{ph}(0, \lambda)\,e^{-\sigma(\lambda)x}$. Approximately,

$$G(x) = G_{eff}\,e^{-\sigma x},$$

where $G_{eff} = \sigma(\lambda)\,\Phi_{ph}(0, \lambda)$ provided one neglects back reflectance. The optical absorption of the cell depends on the photon wavelength $\lambda_{ave} = 1/\sigma$ (~100 nm) that

accounts for the whole solar spectrum (σ can be considered as the optical absorption coefficient) and should be understood as the average optical decay length. It is noticed that by applying the transfer matrix method, the position-dependent photon absorption can be determined [25] (here qG_{max} = 23 mA/cm^2) gives the maximum absorption $G_{max} = G_{eff}\ \lambda_{ave}$.

The Poisson equation has the form

$$\partial^2\phi/\partial x^2 = -\rho/\epsilon,$$

where ϕ is the electric potential, ρ is charge distribution, and ϵ is the permittivity of the medium.

Assuming that the absorber is intrinsic (so that ρ = 0), the solution of the Poisson equation gives $\phi(x) = ax$ where a is a constant and found by the boundary conditions. Since the voltage drops primarily across the absorber layer, for the p-i-n cells as in fig. 2a, $\phi(x) = 0$ for $x = 0$ and $\phi(x) = V_{bi} - V$ for $x = d$ (note here that as $x = 0$, $V_{bi} = V$). Therefore, $a = (V_{bi} - V)/d$, thus, the electric field reads

$$E = -d\phi/dx = (V - V_{bi})/d.$$

where d is the absorber thickness and V_{bi} is the built-in potential across the absorber that is mainly specified by the doping of the selective transport layers as well as the band alignment at the interface (see fig. 2).

Inserting $G(x)$ and E into Eqs. (5) and (6), we obtain their solutions given by

$$n(x) = n_o + e^{-\varepsilon x/2}\,[A_n \cosh(\alpha_n x/2) + B_n \sinh(\alpha_n x/2)] + \gamma_n\, e^{-\sigma x}, \quad (7)$$

$$p(x) = p_o + e^{-\varepsilon x/2}\,[A_p \cosh(\alpha_p x/2) + B_p \sinh(\alpha_p x/2)] + \gamma_p\, e^{-\sigma x}, \quad (8)$$

where $\varepsilon \equiv qE/kT$ is the normalized electric field, parameters α and γ are given

$$\alpha_n = (4/L_n^2 + \varepsilon^2)^{1/2},$$
$$\alpha_p = (4/L_p^2 + \varepsilon^2)^{1/2},$$
$$\gamma_n = L_n^2\, G_n/[1 + \sigma\, L_n^2(\varepsilon - \sigma)],$$
$$\gamma_p = L_p^2\, G_p/[1 - \sigma\, L_p^2(\varepsilon + \sigma)],$$

$G_n \equiv G_{eff}/D_n$ and $G_p \equiv G_{eff}/D_p$ represent the normalized generation rates, $L_n = (D_n\ \tau_n)^{1/2}$ and $L_p = (D_p\ \tau_p)^{1/2}$ the diffusion lengths of electrons and holes, A_n (A_p) and B_n (B_p) are constants determined by the boundary conditions as given in figure 3 [15], where the effective doping concentration $N_{A,eff}$ (acceptor) and $N_{D,eff}$ (donor) are the equilibrium hole and electron concentrations at the ends of the i-layer. Because the electron affinities and the doping will decide the concentrations, the built-in potential is

$$V_{bi} = (kT/q)\ \ln(N_{A,eff}N_{D,eff}/n_i^2),$$

and s_n and s_p are the minority carrier surface recombination velocities.

Applying the boundary conditions, A_n, A_p, and B_n, B_p will be determined, then input them to Eqs. (3) and (4) to get the current density:

$$J = J(0) = J_n(0) + J_p(0).$$

Hence, we can divide the current into two parts, a voltage-dependent photo-current J_{photo} and a dark diode J_{dark} (independent of generation),

$$J_{light} = J_{photo} + J_{dark}.$$

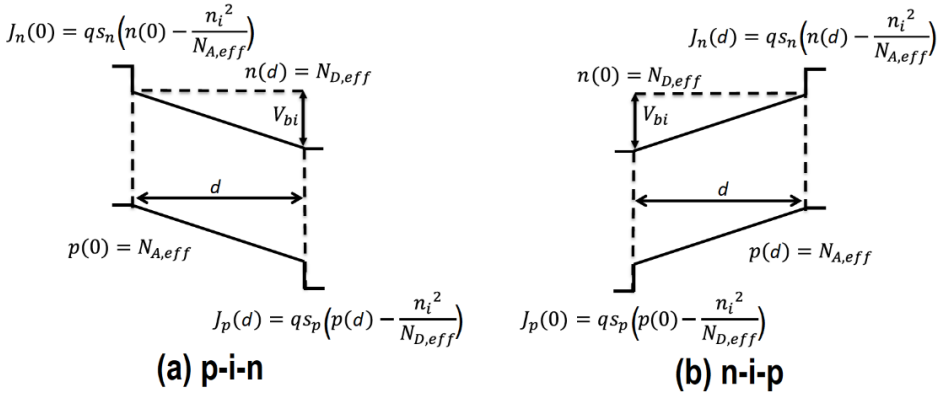

Figure 3. *The boundary conditions labeled in the energy diagram of (a) p-i-n type and (b) n-i-p type PSCs.*

In order to validate the model, we fit both light and dark J-V characteristics for two different perovskite cells using the model, as shown in fig. 2. The inputting parameters taken for the two samples #1 and #2 are listed in table 1. With this attractive physics model, the critical parameters of the J-V characteristics of very different cell geometries as well as the known physical parameters of the cell (e.g., the thickness of the absorber) can be easily provided.

Table 1. *Inputting physical parameters of samples #1 (p-i-n type) and #2 (n-i-p type).*

Type	V_{bi} (eV)	d (nm)	D_n (cm^2/s)	D_p (cm^2/s)	μ_n (cm^2/Vs)	μ_p (cm^2/Vs)	τ_n (ns)	τ_p (ns)	n_o	p_o	N_A	N_D	s_n (cm/s)	s_p (cm/s)
p-i-n	1	400	0.05	0.03	0.1	0.2	30	20	10^{15}	10^{16}	10^{17}	10^{19}	10^3	10^2
n-i-p	1	400	0.05	0.03	0.1	0.2	30	20	10^{15}	10^{16}	10^{17}	10^{19}	10^4	10^3

3. SIMULATION RESULTS AND DISCUSSION

We adopt the general drift-diffusion equations, combined with the continuity and the Poisson equations for both electrons and holes that have been described in the last section. We add the specific recombination model and boundary conditions that apply to the given problem according to the interface properties and then run a numerical simulation, which will provide the band-bending, electron and hole concentrations, and currents.

At the start of the simulation, structure parameters of the cell should be provided, such as PEDOT: PSS/Perovskite/PCBM or TiO2/Perovskite/Spiro-OMeTAD. And the absorber is clarified as self-doped or not. After that, the initial value set will be estimated and provided. Additionally, the limited range of each parameter also is clarified.

During the simulation, the physical parameters that are deduced are G_{max}, σ, d, D_n, D_p, τ_n, τ_p, s_n, s_p, V_{bi}, N_A and N_D, that are initially taken from Ref. [26] for the sample #1 (p-i-n) and from [27] for the sample #2 (n-i-p) as extracted in the table 1. Where qG_{max} can be achieved by integrating the photon absorption (it gives around 23 mA/cm^2) and σ is calculated by λ_{ave} around 100 nm; D_n and D_p are

about 0.05 cm^2/s for the material system. Since the absorber thickness is around 300 nm to 500 nm for perovskite solar cells, about 400 nm is a sensible initial guess for d. Due to low carrier lifetime in TiO_2 and a low insufficient barrier between PEDOT:PSS and perovskites so in most cases, s_n is greater than s_p. Hence, the initial guesses for s_n and s_p could be approximated as 10^3 cm/s and 10^2 cm/s, respectively. Finally, the built-in junction V_{bi} is estimated to be the cross-over voltage of dark and light J-V curves.

The results of both dark and light J-V characteristics for two different perovskite cells using the model, as shown in fig. 4. Note that sample #1 has the higher fill-factor (FF), but its V_{oc} is 0.05 V smaller than that of #2 as depicted in fig. 5. The reduction in V_{oc} can be explained by lower built-in potential V_{bi} and higher significant surface recombination velocity $J_{no(po)} = qs_{n(p)} |\Delta n(p)|$. The fill-factor for sample #2 is lower since the velocities of the surface recombination at both contacts are relatively high effective.

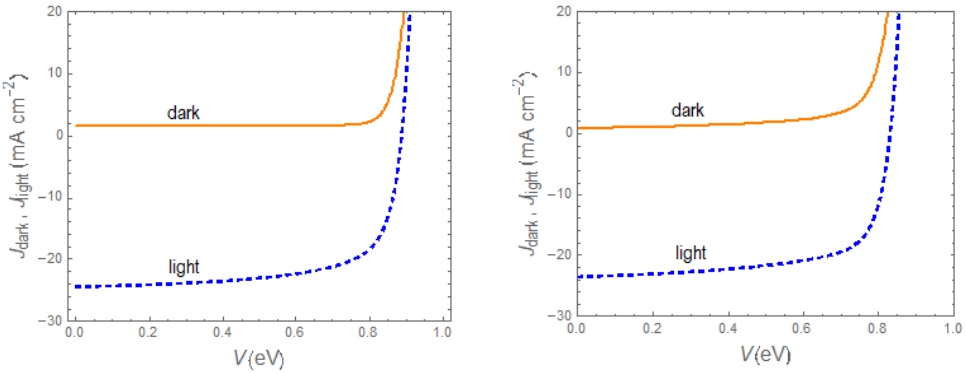

Figure 4. *Characteristics of dark J-V (solid line) and light J-V (dashed line) for (a) p-i-n type and (b) n-i-p type. The parameters are summarized in table 1.*

One of the most questions is that what factors are essential to improve the efficiency of PCS when the physical parameters for high-efficiency samples (#1 and #2) with essentially intrinsic absorbers are provided. It is obvious to point out that this model can help to establish the efficiency of the PCS as a function of various parameters. The dependence of cell efficiency on absorber thickness will be explored as an example as seen in fig. 5 (notice that the values of other parameters will be the same in table 1). Our model shows that, though there is incomplete absorption, both samples have their optimal thickness. In fig. 5a, absorber has the highest efficiency as 100 nm < d < 150 nm (for p-i-n type) and 50 nm < d < 70 nm (for n-i-p type). The efficiency decreases as the absorber thickness is less or greater than these values. A thinner absorber cannot absorb light completely, then the concentration of electrons and holes is too low to generate the currents, while a thicker absorber suppresses charge collection and degrades the fill factor, the recombination happens more frequently, and the concentration of electrons and holes decreases. This result can be explained as the competition between the electric field, and the surface recombination decides the carrier collection efficiency near the interface, and the electric field decreases vs. the thickness.

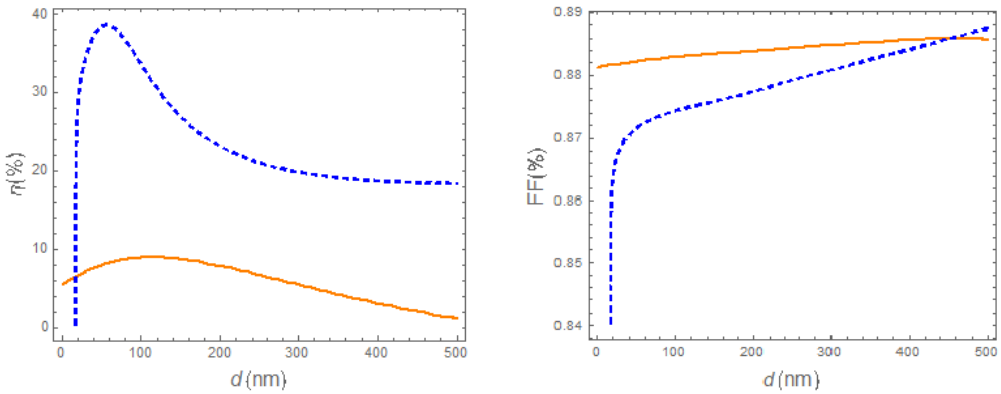

Figure 5. *(a) Efficiency vs. absorber thickness for p-i-n type (solid red line) and n-i-p type (dashed blue line). (b) Fill factor vs. absorber thickness for p-i-n type (solid red line) and n-i-p type (dashed blue line).*

Similarly, we can investigate the dependence of device currents and efficiencies on absorber thickness, temperature, and the built-in potential as seen in figs 6, 7, 8, and 9, respectively (it is also noticed that values of other parameters are the same in table 1).

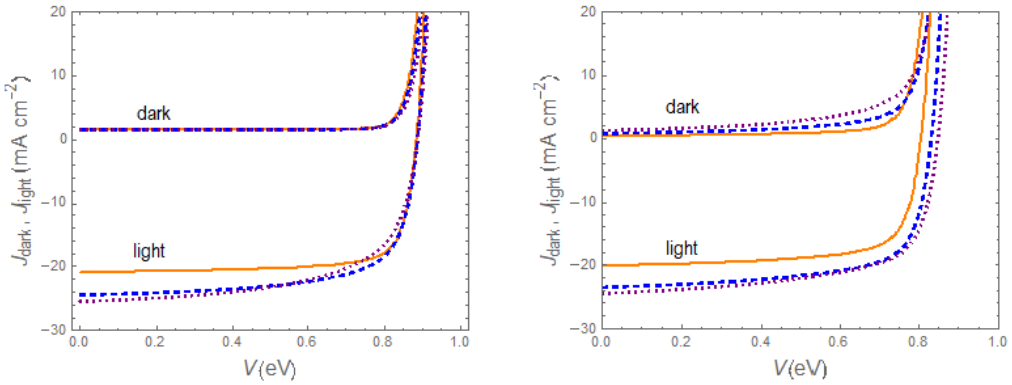

Figure 6. *Characteristics of dark JV and light JV for (a) p-i-n type and (b) n-i-p type for different absorber thickness 200 nm (solid lines), 400 nm (dashed lines), 600 nm (dotted lines).*

The results show that the maximum power and the power conversion efficiency decrease as increasing temperature and/or decreasing built-in potential. The results are similar to external and internal quantum efficiencies (EQE and IQE), as shown in figs. 10 and 11. The combination of light-harvesting, charge generation, and charge collection phenomena, including recombination effects, determine the photovoltaic EQE. The EQE_{PV} is the central function that establishes the practical value of the photo-current. It also determines the fundamental operation properties of the solar cell. The internal quantum efficiency (IQE) is the probability that an excited molecule or an electron-hole pair recombines radiatively. IQE_{PV} is the flux of collected electrons per photon absorbed.

Our model suggests that in order to improve the solar cell performance, we should design the solar cells with a thickness of absorber near to the optimal value,

with a built-in potential high enough, and use them in an environment with a low enough temperature.

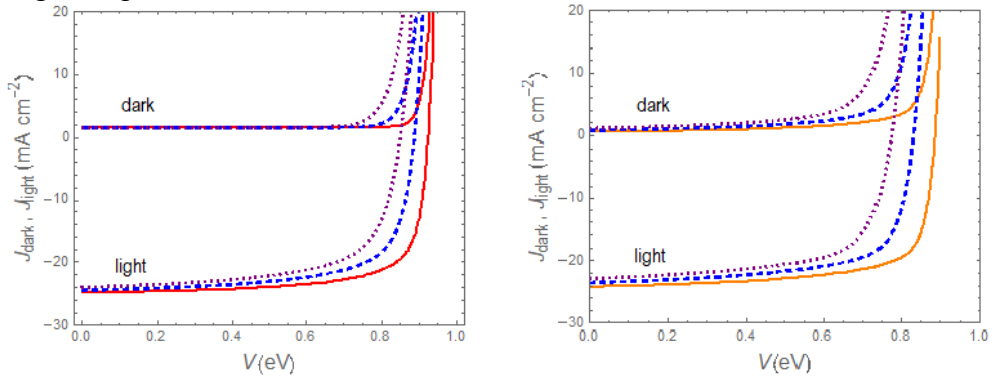

Figure 7. *Characteristics of dark JV and light JV for (a) p-i-n type and (b) n-i-p-type for different temperatures, 200 K (solid lines), 300 K (dashed lines), and 400 K (dotted lines).*

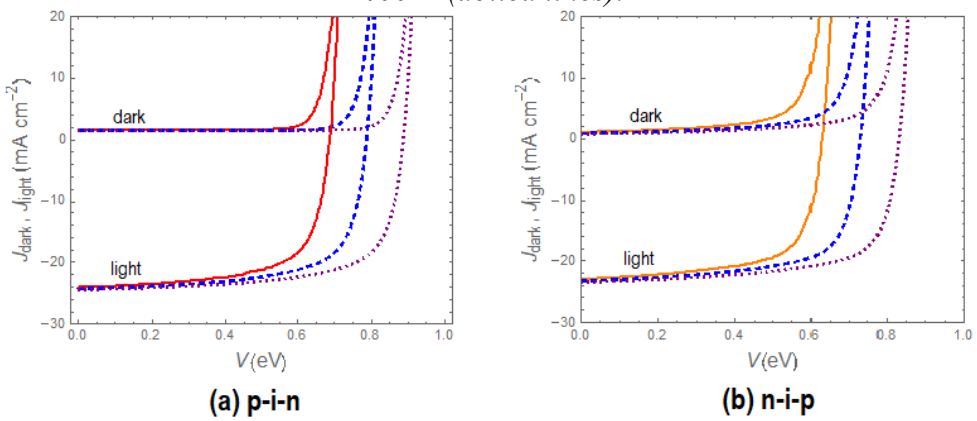

Figure 8. *Characteristics of dark JV and light JV for (a) p-i-n type and (b) n-i-p type for different built-in potential, 0.8 V (solid lines), 0.9 V (dashed lines), and 1 V (dotted lines).*

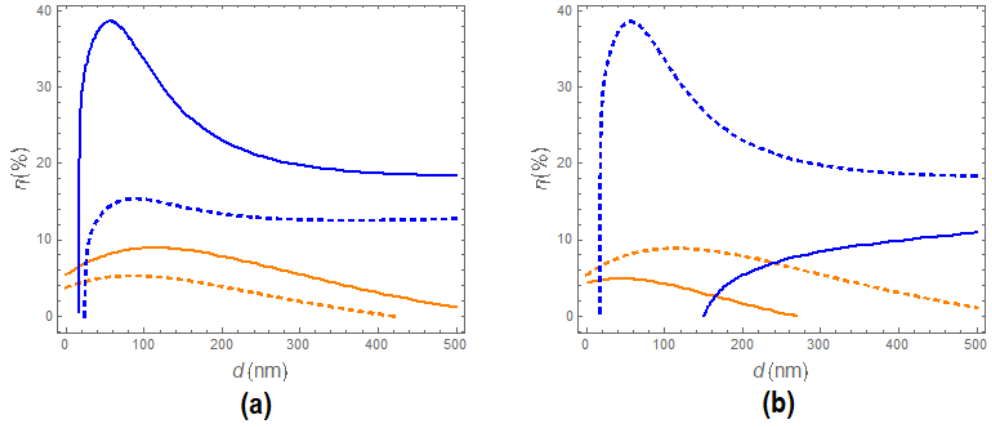

Figure 9. *Efficiency vs. absorber thickness for p-i-n type (red line) and n-i-p type (blue line) for (a) different temperature: 300 K (solid line) and 400 K (dashed line), and for (b) different built-in potential: 0.9 V (solid line) and 1 V (dashed line).*

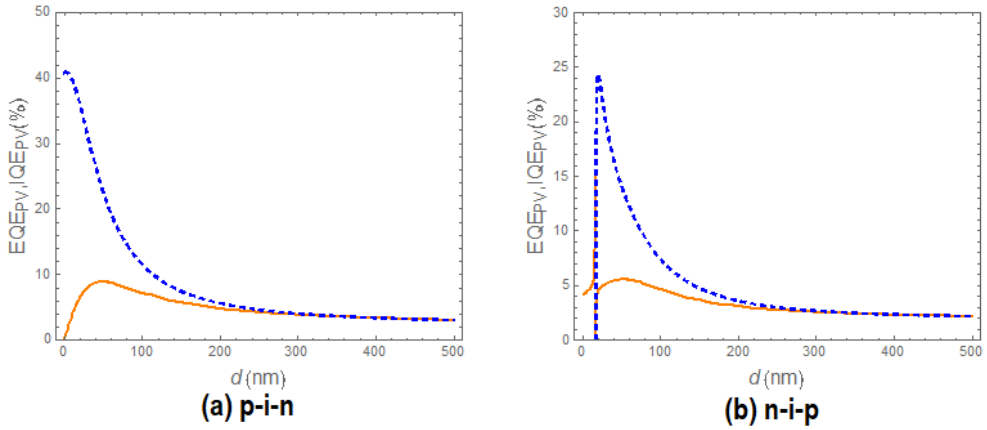

Figure 10. *External quantum efficiency (solid red lines) and internal quantum efficiency (dashed blue lines) vs. absorber thickness for p-i-n type (a) and n-i-p type (b).*

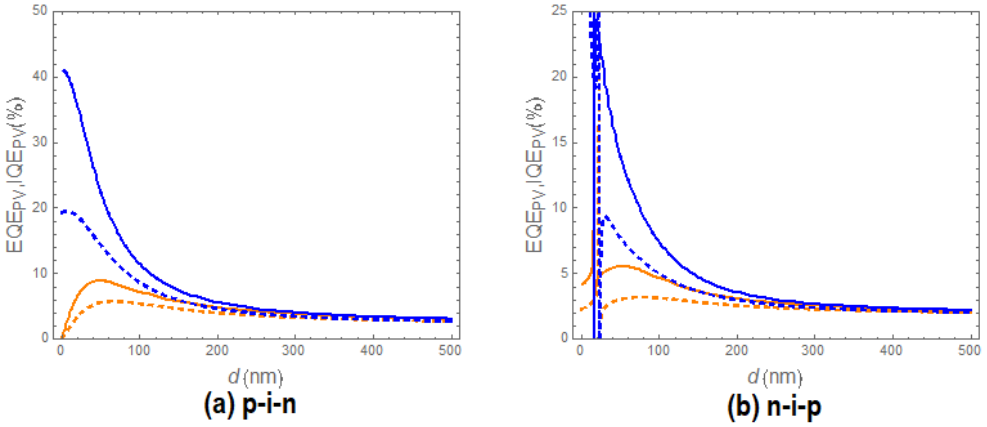

Figure 11. *External quantum efficiency (red lines) and internal quantum efficiency (blue lines) vs. absorber thickness for p-i-n type (a) and n-i-p type (b) for different temperatures: 300 K (solid lines) and 400 K (dashed lines).*

4. CONCLUSIONS

Our model gives useful results on both dark and light current-voltage characteristics as well as power and quantum efficiencies for two different traditional types (p-i-n and n-i-p) of perovskite solar cells. Some other interesting results are also showed since we consider the dependence of the model on temperature, the built-in potential, and the absorber thickness. The change of results can be easily observed as any parameter alters.

A significant merit of this developed model is that, along with simulation techniques, it develops of [15] for accounting to recombination but still offering a simple and complementary way to characterize, screen, and optimize fabricated cells. By simulating this developed model, several physical parameters without directly measured, for example, V_{bi} of a p-i-n device, can be adjusted.

Our model gives a complete figure of a solar cell, and it suggests opportunities for further improvements, such as the estimation of the ultimate performance of the

PCS modules or panels. Developing the physics-based analytical model by accounting for carrier recombination within the absorber layer ($R \neq 0$) and closing the cell-to-module gap are promising next studies and an essential pre-requisite for the commerce of PCS. This may be one of the topics for our further study.

REFERENCES

[1]. Mitzi D. B., Wang S., Feild C. A., Chess C. A., and Guloy A. M. – *"Conducting layered organic–inorganic halides containing <110>-oriented perovskite sheet"*, Science **267** (1995) 1473.

[2]. Mitzi D. B., Chondroudis K., and Kagan C. R. – *"Organic-inorganic electronics"*, IBM J. Res. Dev. **45** (2001) 29.

[3]. Kojima A., Teshima K., Miyasaka T., and Shirai Y. – *"Novel photoelectrochemical cell with mesoscopic electrodes sensitized by lead-halide compounds (2)"*, in Proc. 210th ECS Meeting (ECS, 2006).

[4]. Kojima A., Teshima K., Shirai Y., and Miyasaka T. – *"Organometal halide perovskites as visible-light sensitizers for photovoltaic cells"*, J. Am. Chem. Soc. **131** (2009) 6050.

[5]. Lee M. M., Teuscher J., Miyasaka T., Murakami T. N., and Snaith H. J. – *"Efficient hybrid solar cells based on meso-superstructured organometal halide perovskites"*, Science **338** (2012) 643.

[6]. Kim H.-S., Lee C.-R., Im J.-H., Lee K.-B., Moehl T., Marchioro A., Moon S.-J., Humphry-Baker R., Yum J.-H., Moser J. E., Gratzel M., and Park N.-G. – *"Lead iodide perovskite sensitized all-solid-state submicron thin film mesoscopic solar cell with efficiency exceeding 9%"*, Sci. Rep. **2:591** (2012) 1.

[7]. Correa-Baena J.-P., Abate A., Saliba M., Tress W., Jacobsson T. J., Gratzel M., and Hagfeldt A. – *"The rapid evolution of highly efficient perovskite solar cells"*, Energy Environ. Sci. **10** (2017) 710.

[8]. Niu G., Guo X., and Wang L. – *"Review of recent progress in chemical stability of perovskite solar cells"*, J. Mater. Chem. A **3** (2015) 8970.

[9]. Stranks S. D. and Snaith H. J – *"Metal-halide perovskites for photovoltaic and light-emitting devices"*, Nat. Nanotechnol. **10** (2015) 391.

[10]. Minemoto T. and Murata M. – *"Impact of work function of back contact of perovskite solar cells without hole transport material analyzed by device simulation"*, Curr. Appl. Phys. **14** (11) (2014) 1428.

[11]. De Angelis F. – *"Modeling Materials and Processes in Hybrid/Organic Photovoltaics: From Dye-Sensitized to Perovskite Solar Cells"*, Acc. Chem. Res. **47** (11) (2014) 3349.

[12]. Minemoto T. and Murata M., *"Theoretical analysis on effect of band offsets in perovskite solar cells,"* Sol. Energy Mater. Sol. Cells **133** (2015) 8.

[13]. Tripathi B., Bhatt P., Chandra Kanth P., Yadav P., Desai B., Kumar Pandey M., and Kumar M., *"Temperature induced structural, electrical and optical changes in solution processed perovskite material: Application in photovoltaics,"* Sol. Energy Mater. Sol. Cells **132** (2015) 615.

[14]. Foster J. M., Snaith H. J., Leijtens T., and Richardson G., *"A model for the operation of perovskite-based hybrid solar cells: formulation, analysis and comparison to experiment,"* SIAM J. Appl. Math., **74**(6) (2014) 1935.

[15]. Sun X., Asadpour R., Nie W., Mohite A. D., Alam M. A., *"A Physics-based Analytical Model for Perovskite Solar Cells,"* IEEE Journal of Photovoltaics **5**(5) (2015) 1389.
[16]. Hejri M., Mokhtari H., Azizian M. R., Ghandhari M., and Soder L., *"On the Parameter Extraction of a Five-Parameter Double-Diode Model of Photovoltaic Cells and Modules,"* IEEE J. Photovoltaics **4**(3) (2014) 915.
[17]. Ishaque K., Salam Z., and Taheri H., *"Simple, fast and accurate two-diode model for photovoltaic modules,"* Sol. Energy Mater. Sol. Cells **95**(2) (2011) 586.
[18]. Dongaonkar S. and Alam M. A., *"End to end modeling for variability and reliability analysis of thin film photovoltaics,"* in Proc. IEEE International Reliability Physics Symposium (2012).
[19]. Dongaonkar S., Deline C., and Alam M. A., *"Performance and reliability implications of two-dimensional shading in monolithic thin-film photovoltaic modules,"* IEEE J. Photovoltaics **3**(4) 2013) 1367.
[20]. Brecl K. and Topič M., *"Simulation of losses in thin-film silicon modules for different configurations and front contacts,"* Prog. Photovoltaics Res. Appl. **16**(6) (2008) 479.
[21]. Brecl K., Topič M., and Smole F., *"A detailed study of monolithic contacts and electrical losses in a large-area thin-film module,"* Prog. Photovoltaics Res. Appl. **13**(4) (2005) 297.
[22]. Koishiyev G. T. and Sites J. R., *"Impact of sheet resistance on 2-D modeling of thin-film solar cells,"* Sol. Energy Mater. Sol. Cells. **93**(3) (2009) 350.
[23]. Zhang L., *"Device physics of perovskite solar cells,"* Ph.D. Theses, Iowa State University (2017).
[24]. Bisquert J., *"The Physics of Solar Cells: Perovskites, Organics, and Photovoltaic Fundamentals,"* CRC Press, Taylor & Francis Group, FL, USA (2018).
[25]. Pettersson L. A. A., Roman L. S., Inganäs O., and Inganäs O., *"Modeling photo-current action spectra of photovoltaic devices based on organic thin films,"* J. Appl. Phys. **86**(1) (1999) 487.
[26]. Nie W., Tsai H., Asadpour R., Blancon J.-C., Neukirch A. J., Gupta G., Crochet J. J., Chhowalla M., Tretiak S., Alam M. A., Wang H.-L., and Mohite A. D., *"High-efficiency solution-processed perovskite solar cells with millimeter-scale grains,"* Science **347**(6221) (2015) 522.
[27]. Liu M., Johnston M. B., and Snaith H. J., *"Efficient planar heterojunction perovskite solar cells by vapour deposition.,"* Nature **501**(7467) (2013) 395.
[28]. Di Giacomo F., Zardetto V., D'Epifanio A., Pescetelli S., Matteocci F., Razza S., Di Carlo A., Licoccia S., Kessels W. M. M., Creatore M., and Brown T. M., *"Flexible Perovskite Photovoltaic Modules and Solar Cells Based on Atomic Layer Deposited Compact Layers and UV-Irradiated TiO 2 Scaffolds on Plastic Substrates,"* Adv. Ener. Mater. **5**(8) (2015) 1401808.
[29]. Matteocci F., Cinà L., Di Giacomo F., Razza S., Palma A. L., Guidobaldi A., D'Epifanio A., Licoccia S., Brown T. M., Reale A., and Di Carlo A., *"High efficiency photovoltaic module based on mesoscopic organometal halide perovskite,"* Prog. Photovoltaics Res. Appl. **20**(1) (2014) 6.

TÓM TẮT

XÂY DỰNG MÔ HÌNH VẬT LÝ CỦA TẤM PIN NĂNG LƯỢNG MẶT TRỜI VỚI VẬT LIỆU PEROVSKITE

Perovskites ngày càng được chứng minh là một loại vật liệu đầy hứa hẹn trong việc chế tạo vật liệu hấp thụ cho pin mặt trời thế hệ tiếp theo với hiệu quả cao và chi phí thấp. Có một số mô hình được đề xuất cho pin mặt trời perovskite tương tự như pin mặt trời thông thường, hoạt động của chúng cũng có những đặc điểm cụ thể và yêu cầu phát triển một mô hình vật lý tổng quát hơn để nghiên cứu, do đó tối ưu hóa các tế bào và cải thiện hiệu suất của các tấm pin. Bài báo này phát triển một mô hình trực quan dựa trên vật lý để xem xét hiệu suất của hai loại pin mặt trời perovskite hiệu quả cao, có tính đến các đặc tính không đồng nhất, với các lớp vận chuyển được lọc, tái tổ hợp, lựa chọn điện tích và bộ thu phụ thuộc điện áp. Mô hình này sẽ cho phép ước tính thực nghiệm các thông số chính của pin mặt trời perovskite, hiểu được nút thắt cổ chai về hiệu suất và dự đoán hiệu suất của pin mặt trời perovskite và đề xuất nghiên cứu thêm để phát triển công nghệ pin mặt trời perovskite.

Từ khóa: Perovskites; Pin mặt trời; Mô hình vật lý.

Received 27th August 2020
Revised 21th September 2020
Accepted 16th November 2020

Author affiliations:
Department of Renewable Energy, Faculty of Energy Technology, Electric Power University.
*Corresponding author: ducnh@epu.edu.vn.